Visible-Light Imaging of the Super-Alfvénic/Sonic Collisional Merging Process of Field-Reversed Configurations with a Contrast Medium-Mixed Plasmoid*)

Daichi KOBAYASHI, Taichi SEKI, Tomohiko ASAI, Keisuke HIRAMA, Reiji HAYATA, Kota ARAOKA, Tsutomu TAKAHASHI and Jordan MORELLI[1)]

College of Science and Technology, Nihon University, Tokyo 101-8308, Japan

[1)]*Department of Physics, Engineering Physics & Astronomy, Queen's University, Kingston, Ontario K7L 3N6, Canada*

(Received 9 January 2023 / Accepted 4 April 2023)

The collisional merging formation process of field-reversed configurations (FRCs) was observed by using a recently developed spectroscopy system. The shape and boundary of the two plasmoids during the merging process were visualized by the "contrast medium" mixing. One of the two initial plasmoids captured a small amount of contrast medium (e.g., helium) diffused in a part of the vacuum vessel during the translation process. The contrast medium-mixed plasmoid merged with the other plasmoid which is without a contrast medium. The contrast-enhanced shape and internal structure of two plasmoids were observed using the spectroscopic systems with the line spectrum of the contrast medium ion. The emission distribution of the contrast medium ions inside the plasmoid was verified by visible-light computed tomography, which revealed that the contrast medium ions were captured only inside one plasmoid. In addition, the emission distribution resembled the density profile in the rigid rotor model, which is a pressure equilibrium model of FRCs. After the collision, the contrast medium ions diffused into the other side. This suggests the beginning of the merging with the plasmoid on the other side. The optically evaluated timescale of the merging was comparable with that observed by the internal magnetic measurements.

Keywords: field-reversed configuration, high beta plasma, FRC merging, spectroscopic imaging, magnetic reconnection

DOI: 10.1585/pfr.18.2402043

1. Introduction

A field-reversed configuration (FRC) is a magnetically confined system that realizes plasma confinement with an extremely high beta. Ideally, an FRC has only poloidal magnetic flux, and the plasma pressure and the external magnetic pressure are completely balanced [1, 2].

In contrast to conventional methods, such as field-reversal theta pinch, the collisional merging formation is a method that can form high-performance FRCs. The collisional merging formation of FRCs has been conducted on the FRC amplification via translation-collisional merging (FAT-CM) device at Nihon University [3] and a series of C-2 devices at TAE Technologies, Inc. [4]. An FRC is again attracting attention as a high-efficiency fusion reactor core plasma because the quasi-steady state sustainment of FRC confinement over 30 ms has been achieved in experiments on the C-2U/W device [5]. In the collisional merging formation of FRCs, two initially formed FRC-like plasmoids are accelerated by a magnetic pressure gradient toward each other. The relative speed just before the collision exceeds both the typical Alfvén speed and ion sound speed at the separatrix [6]. A single FRC is formed by the collision and merging of the two plasmoids. The observation of the merging process is being attempted on the FAT-CM device. Internal magnetic measurements observed that the merging process is completed in several tens of microseconds [7]. This timescale is much faster than that predicted by a two-dimensional resistive magnetohydrodynamics (MHD) simulation without an artificial adjustment in resistivity. This suggests a breakdown of the MHD approximation in this process. In the super-Alfvénic/sonic merging process accompanied by shock wave excitation, it can be considered that some physical mechanisms, such as the current drive by the rapid production of a steep pressure gradient, can be considered to contribute to the fast merging.

In this work, visible-light imaging using a fast-framing camera and tomography system was attempted to evaluate the internal structure of the initial-plasmoid and the timescale of the merging process without the perturbation of plasma performance.

author's e-mail: kobayashi.daichi@nihon-u.ac.jp

*) This article is based on the presentation at the 31st International Toki Conference on Plasma and Fusion Research (ITC31).

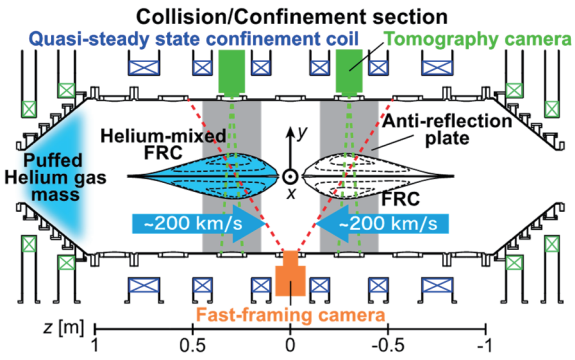

Fig. 1 Illustration of collision and confinement section of FAT-CM device.

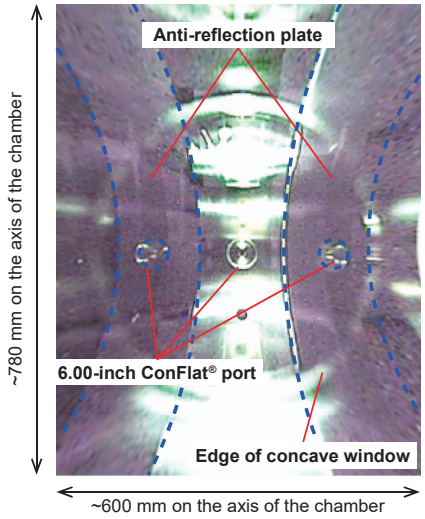

Fig. 2 Real color image in the field of view of the fast-framing camera without a bandpass filter and plasma. Blue dashed lines denote the shape of anti-reflection plates.

2. Experimental Setup

The FAT-CM device consists of two formation and acceleration sections and the collision and confinement section. Figure 1 shows an illustration of the collision and confinement section. Initial plasmoids, which were formed at both the formation and acceleration sections, were accelerated by a magnetic pressure gradient and translated into the collision and confinement section. The typical translation speed was 100 - 200 km/s. The typical electron density and ion temperature of the plasmoid, and the external magnetic field were 2×10^{20} m^{-3}, 80 eV, and 0.05 T, respectively. Therefore, the Alfvén Mach and ion Mach numbers for the translation speed were in the range of 2 to 4.

The translation and merging processes were observed by using a visible-light tomography camera system [8, 9] and a fast-framing camera-based spectroscopy system [10]. The tomography camera system consists of a cylindrical lens (LK1816L1-A, Thorlabs, Inc.), slit, bandpass filter, and multi-anode photomultiplier tube (PMT) (R5900U-07-L16, Hamamatsu Photonics K.K.). Observation on the order of microseconds was realized using the PMT as a sensor. The emission light from the plasma in the field of view, expanded by the cylindrical lens, passes through the slit and bandpass filter and enters the PMT. The internal emission distribution of the plasma can be obtained by tomographic imaging using the line-of-sight information for each channel of the PMT and the observed signals. The fast-framing camera (ULTRA Cam HS-106E, nac Image Technologies, Inc.) was utilized for the spectroscopy system. The camera can observe the merging process on the order of microseconds because the fastest frame rate is 1.25 MFPS, and the shutter speed can be shortened to 0.1 µs. A wide field of view was served by using a fish-eye lens (AF DX Fisheye-Nikkor 10.5 mm f/2.8G ED, Nikon Corp.), and the inside of the chamber can be seen widely as shown in Fig. 2. Note that, the anti-reflection plates for the tomography camera were installed at both sides of the midplane as shown in Figs. 1 and 2. The anti-reflection plate has holes that matched the position and size of the measurement ports arranged on the metal chamber axially/azimuthally. The chamber wall (more precisely, the surface of the flange) can be seen through the hole in the anti-reflection plate. In addition, a bandpass filter can be mounted inside the lens. As described in the next section, a bandpass filter for singly ionized helium (center wavelength: 470 nm, full-width half maximum: 10 nm) was used in both systems because helium was used as the contrast medium. Two tomography cameras and the fast-framing camera were installed at $z = \pm 0.3$ m and the midplane, respectively.

3. Contrast Medium Mixing

The initial plasmoids were formed using deuterium gas. Observing the shape and boundary of the two plasmoids and their time evolution using simple spectroscopic measurements is difficult because the two plasmoids have similar light emissions. Therefore, the "contrast medium" was mixed into one of the two plasmoids. Here, helium was used as the contrast medium because the specific charge of helium ions closest to that of deuterium ions. One of the translated plasmoids passed through a helium gas mass locally supplied to the taper part ($z \sim 1.2$ m) of the confinement chamber. Helium was ionized by collision with electrons and/or deuterium ions. The ionized helium was captured by the confinement field of the plasmoid.

4. Experimental Results

4.1 Single-sided translation case

Experiments in which only one initial plasmoid was formed at one of the formation and acceleration sections and was translated (single-sided translation case), were conducted to evaluate the internal structure of the plasmoid during translation. The plasmoid was translated from the left-hand side of Fig. 1. Figure 3 shows the radial pro-

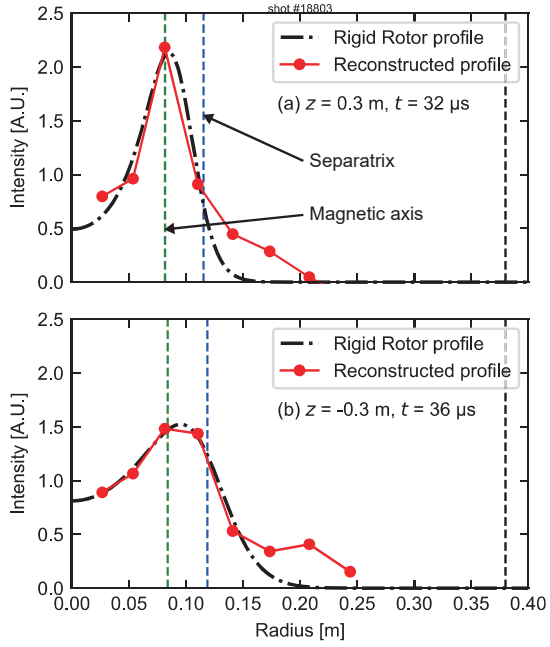

Fig. 3 Radial profile of helium ion emission when the plasmoid passed through (a) $z = 0.3$ m, and (b) $z = -0.3$ m. Green, blue and black dashed lines denote the magnetic axis, separatrix and inner radius of the chamber, respectively.

file of the helium ion emission during translation observed using the tomography camera. The observed optical signals were reconstructed to obtain the radial profile by applying the Abel inversion method [11, 12]. The emission peaks were around the magnetic axis denoted by the green dashed lines. The magnetic axis of an ideal FRC is at the position divided by the square root of two of the separatrix radii denoted by the blue dashed lines. This profile strongly resembles the density profile in the rigid rotor (RR) model [13], which is a the pressure equilibrium model of FRCs. The profile fitted by the RR model is shown as black trend lines in Fig. 3. This result indicates that helium ions were captured not only on the surface of the plasmoid but also inside the plasmoid. It also suggests that the plasmoid retained an FRC-like structure during the super-Alfvénic/sonic translation process. Notably, no emission of helium ions was observed during the translation process when the FRC was translated from the opposite side to the helium supply (from the right-hand side of Fig. 1).

4.2 Collisional merging case

The collisional merging process was observed using the fast-framing camera. Figure 4 shows the images taken by the fast-framing camera with the bandpass filter. The contrast of the images was fixed to enhance the shape of

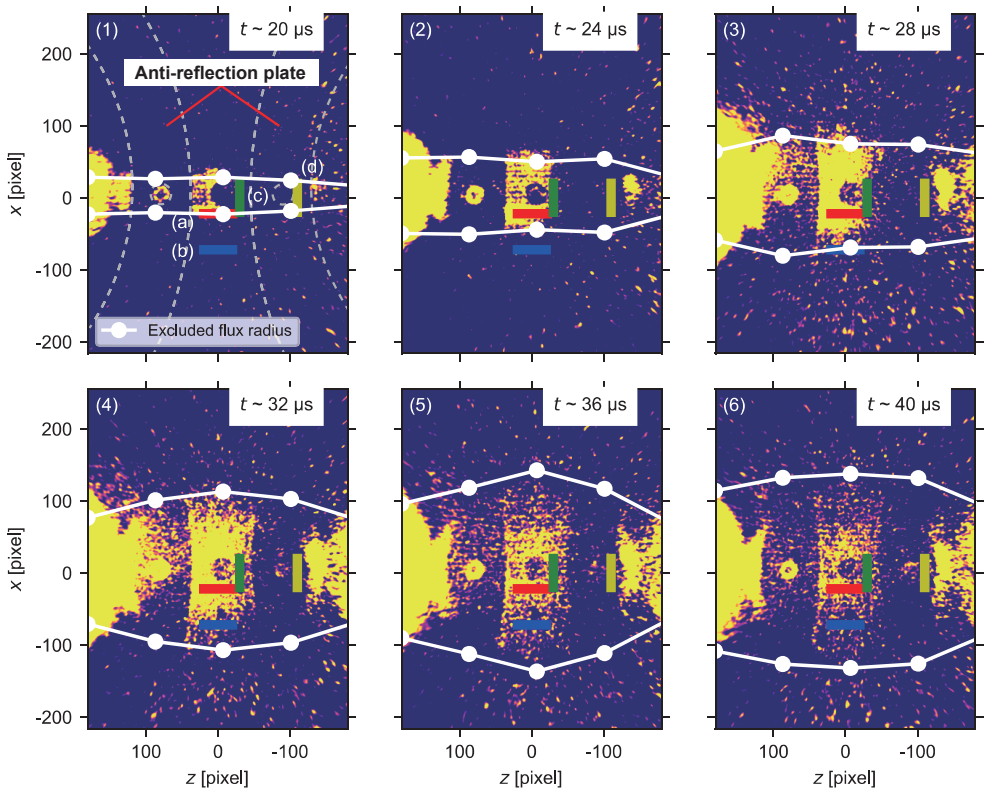

Fig. 4 Contrast fixed images taken at each timing (1) - (6). Yellow area shows helium ion emission. The white dots and lines denote the plasma radius estimated by magnetic measurement. The frame rate and shutter speed were 500 kFPS and open, respectively. Grey dashed lines in image (1) denote the shape of anti-reflection plates.

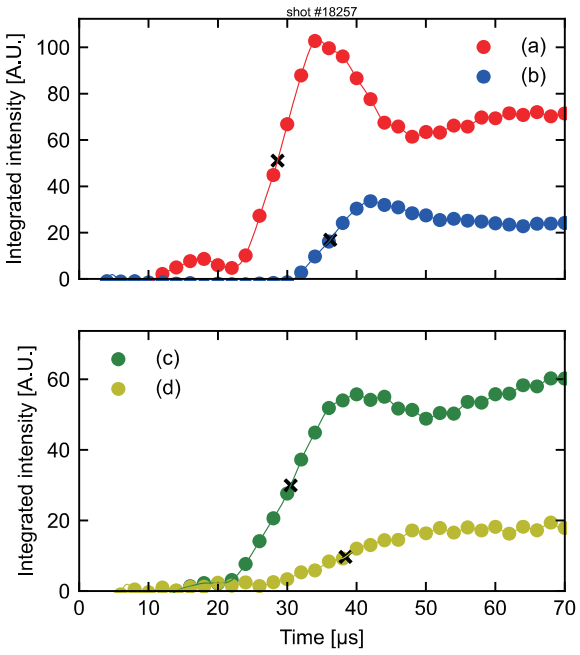

Fig. 5 Time evolution of integrated emission intensity of each region in Fig. 4. Black crosses denote the rise-time, when the intensity reached half of the first peak value in each region.

the plasma. The anti-reflection plates can be seen in the images (approximately $z \sim \pm 100$ pixel). The reflection was reduced in the regions with anti-reflection plates. Although slightly affected by the reflection on the chamber wall, the emission area was localized only inside the plasma radius indicated by the white line. The contrast medium-mixed plasmoid was translated from the left-hand side of the images. The emission area was mainly in the left half of the images in Figs. 4 (1) - (3). The bright emission in the midplane in Figs. 4 (3) and (4) may suggest the shock front and/or current sheet formed by the collision. However, it is also possible that the midplane appears brighter due to reflection on the chamber wall. As shown in Fig. 4 (4) onwards ($t > 30\,\mu$s), the emitting area expanded over the entire plasma volume. As indicated by the tomographic imaging in the single-sided translation case, the captured helium ions were confined inside the plasmoid during the translation process. Assuming that helium ions were localized on each magnetic surface, helium ions did not move to the opposite side unless magnetic reconnection occurred. Therefore, the beginning of the expansion of the emission area indicated the beginning of merging.

The time scale of merging and the outflow speed were estimated from images. Figure 5 shows the time evolution of emission intensity integrated over the regions denoted as (a) red, (b) blue, (c) green, and (d) yellow rectangles in Fig. 4. Black crosses denote the rise-time, when the intensity reached half of the first peak value in each region. The axial (z-direction) and radial (x-direction) speeds of emission area expansion were estimated from the difference in the rise-times and the position of each area. The axial speed was approximately 29 km/s. The axial length of the plasma after merging was approximately 1.8 m. W The time for helium to diffuse throughout the plasma volume was defined as the time to complete merging, and it was obtained as 31 μs from the half length of the plasma and the axial speed. This timescale is comparable to the timescale until the FRC-like magnetic field is reformed as observed by internal magnetic measurements [3, 7]. The radial speed was approximately 15 km/s. This value is on the order of the Alfvén speed (~50 km/s on the separatrix). Therefore, the radial speed would be the outflow speed by reconnection.

5. Summary

The shape and boundary of two initial plasmoids during the super-Alfvénic/sonic collisional merging process were successfully visualized by the developed spectroscopic observation technique with the contrast medium-mixed plasmoid. The FRC-like structure of the initial plasmoids was observed to be retained without a perturbation during the super-Alfvénic/sonic translation process. In addition, the timescale of the merging estimated from the observed images is comparable to that observed by internal magnetic measurements. This result is evidence of the considerably faster FRC merging than predicted by MHD approximation, and it is also suggested by internal magnetic measurements.

A shockwave should be excited by the collision of the initial plasmoids because the Alfvén/ion Mach number during translation is 2 - 4. In addition, the radial size parameter S ($\equiv R/\rho_i$) [2] is 1 - 2. Here, R and ρ_i are the radius of the magnetic axis and the ion Larmor radius, respectively. The ion Larmor radius is comparable to the plasma size in this work. These observations suggest that shock heating and the finite Larmor radius effect may contribute to the fast merging. However, additional observations on these effects are necessary to evaluate the mechanisms of the fast merging fully.

Acknowledgments

The authors gratefully acknowledge the support of nac Image Technology Inc. This work was partially supported by JSPS KAKENHI Grant No. JP20H00143 and the Grant for External Fund Acquisition (Startup) Support, Grant for Project Research, and the Grant for the Promotion of Leading Research, College of Science and Technology, Nihon University.

[1] M. Tuszewski, Nucl. Fusion **28**, 2033 (1988).
[2] L.C. Steinhauer, Phys. Plasmas **18**, 070501 (2011).
[3] T. Asai, D. Kobayashi, T. Seki, Y. Tamura, T. Watanabe *et al.*, Nucl. Fusion **61**, 096032 (2021).
[4] M.W. Binderbauer, H.Y. Guo, M. Tuszewski, S. Putvinski, L. Sevier *et al.*, Phys. Rev. Lett. **105**, 045003 (2010).

[5] H. Gota, M.W. Binderbauer, T. Tajima, A. Smirnov, S. Putvinski *et al.*, Nucl. Fusion **61**, 106039 (2021).
[6] D. Kobayashi and T. Asai, Phys. Plasmas **28**, 022101 (2021).
[7] T. Asai, T. Takahashi, J. Sekiguchi, D. Kobayashi, S. Okada *et al.*, Nucl. Fusion **59**, 056024 (2019).
[8] H. Tomuro, T. Asai, K. Iguchi, T. Takahashi and Y. Hirano, Rev. Sci. Instrum. **81**, 10E525 (2010).
[9] T. Seki, T. Yamanaka, T. Asai, D. Kobayashi, T. Takahashi *et al.*, Rev. Sci. Instrum. **93**, 103520 (2022).
[10] D. Kobayashi, T. Seki, T. Asai, T. Takahashi J. Morelli *et al.*, Rev. Sci. Instrum. **93**, 103526 (2022).
[11] W. Lochte-Holtgreven *Plasma Diagnostics* (AIP press, New York, 1995) p. 184.
[12] T. Takahashi, H. Gota, T. Fujino, M. Okada, T. Asai *et al.*, Rev. Sci. Instrum. **75**, 5205 (2004).
[13] W.T. Armstrong, R.K. Linford, J. Lipson, D.A. Platts and E.G. Sherwood, Phys. Fluids **24**, 2068 (1981).